

Available online at [www.sciencedirect.com](http://www.sciencedirect.com)

Biochimica et Biophysica Acta 1768 (2007) 2578–2585

[www.elsevier.com/locate/bbamem](http://www.elsevier.com/locate/bbamem)

# Action mechanism of PEGylated magainin 2 analogue peptide

Yuichi Imura<sup>a</sup>, Minoru Nishida<sup>b</sup>, Katsumi Matsuzaki<sup>a,\*</sup>

<sup>a</sup> Graduate School of Pharmaceutical Sciences, Kyoto University, Sakyo-ku, Kyoto 606-8501, Japan

<sup>b</sup> Graduate School of Biostudies, Kyoto University, Sakyo-ku, Kyoto 606-8501, Japan

Received 13 April 2007; received in revised form 14 June 2007; accepted 14 June 2007

Available online 22 June 2007

## Abstract

PEGylation is frequently used to improve the efficacy of protein and peptide drugs. Recently, we investigated its effects on the action mechanism of the cyclic  $\beta$ -sheet antimicrobial peptide tachyplesin I isolated from *Tachypleus tridentatus* [Y. Imura, M. Nishida, Y. Ogawa, Y. Takakura, K. Matsuzaki, Action Mechanism of Tachyplesin I and Effects of PEGylation, *Biochim. Biophys. Acta* 1768 (2007) 1160–1169]. PEGylation did not change the basic mechanism behind the membrane-permeabilizing effect of the peptide on liposomes, however, it decreased the antimicrobial activity and cytotoxicity. To obtain further information on the effects of PEGylation on the activities of antimicrobial peptides, we designed another structurally different PEGylated antimicrobial peptide (PEG-F5W, E19Q-magainin 2-amide) based on the  $\alpha$ -helical peptide magainin 2 isolated from the African clawed frog *Xenopus laevis*. The PEGylated peptide induced the leakage of calcein from egg yolk L- $\alpha$ -phosphatidylglycerol/egg yolk L- $\alpha$ -phosphatidylcholine large unilamellar vesicles, however, the activity was weaker than that of the control peptides. The PEGylated peptide induced lipid flip-flop coupled to the leakage and was translocated into the inner leaflet of the bilayer, indicating that PEGylation did not alter the basic mechanism of membrane permeabilization of the parent peptide. The cytotoxicity of the non-PEGylated peptides was nullified by PEGylation. At the same time, the antimicrobial activity was weakened only by 4 fold. The effects of PEGylation on the activity of magainin were compared with those for tachyplesin.

© 2007 Elsevier B.V. All rights reserved.

**Keywords:** Antimicrobial peptide; Magainin 2; PEGylation; Lipid flip-flop; Peptide–lipid interaction; Inner membrane permeabilization

## 1. Introduction

More than 880 antimicrobial peptides have been isolated from plants, insects and animals including humans or predicted from gene sequences [1,2]. These peptides are considered to play

an important role in the innate immunity of their host species. Antimicrobial peptides are promising candidates for novel therapeutic agents because they are effective against antibiotic-resistant bacteria. However, their application is limited to topical use [1,3] because of disadvantages such as plausible antigenicity, a short circulating half-life due to protease digestion, and a rapid clearance from kidney [4,5], and low therapeutic indices in vivo [1,6]. Several attempts have been made to improve the therapeutic indices of antimicrobial peptides, for example, the entrapment of indolicidin in liposomes [7].

Attaching a polyethyleneglycol (PEG) moiety to peptide and protein drugs (PEGylation) is frequently used to improve efficacy in vivo [4]. However, regarding antimicrobial peptides, there had been only one short report about the PEGylation of nisin [8] until our recent paper. We have reported that the  $\beta$ -sheet peptide tachyplesin I forms a toroidal pore and that PEGylation does not alter the basic mechanism of membrane permeabilization of the parent peptide. Despite similar activities against model membranes, the cytotoxicity of tachyplesin I was greatly reduced by PEGylation, although the antimicrobial activity was

**Abbreviations:** Ac-E19Q-MG<sub>a</sub>, Ac-F5W, E19Q-magainin 2-amide; AMEM, Alpha modification of Eagle's medium; C<sub>6</sub>-NBD-PC, 1-palmitoyl-2-[6-[(7-nitrobenz-2-oxa-1,3-diazol-4-yl) amino]caproyl]-L- $\alpha$ -phosphatidylcholine; CD, circular dichroism; CFU, colony forming unit; CHO, Chinese Hamster Ovary; FBS, fetal bovine serum; Fmoc, 9-fluorenylmethoxycarbonyl; HPLC, high-performance liquid chromatography; L/P, lipid-to-peptide molar ratio; LUVs, large unilamellar vesicles; MG, F5W-magainin 2; MIC, minimal inhibitory concentration; MLVs, multilamellar vesicles; NAPB, 10 mM sodium phosphate/100 mM NaCl, pH 7.4 buffer; ONPG, *o*-nitrophenyl- $\beta$ -D-galactoside; PC, egg yolk L- $\alpha$ -phosphatidylcholine; PEG, polyethyleneglycol; PEG-E19Q-MG<sub>a</sub>, PEG-F5W, E19Q-magainin 2-amide; PG, L- $\alpha$ -phosphatidyl-DL-glycerol enzymatically converted from PC; SUVs, small unilamellar vesicles; TSB, tryptic soy broth; WST-1, 2-(4-iodophenyl)-3-(4-nitrophenyl)-5-(2,4-disulfo-phenyl)-2H-tetrazolium, monosodium salt

\* Corresponding author. Tel.: +81 75 753 4521; fax: +81 75 753 4578.

E-mail address: [katsumim@pharm.kyoto-u.ac.jp](mailto:katsumim@pharm.kyoto-u.ac.jp) (K. Matsuzaki).

significantly weakened (32–64 fold). Outer membranes and peptidoglycan layers play an inhibitory role in the permeation of the PEG moiety into cell membranes [9].

Although PEGylation decreased biological activities of tachyplesin I, a question still remains: whether the results are general to antimicrobial peptides or are specific for the peptide. To obtain further information about the effects of PEGylation, we designed another structurally different PEGylated antimicrobial peptide based on magainin 2. Magainin 2 was isolated from the African clawed frog *Xenopus laevis* (Fig. 1) [10] and is one of the most studied  $\alpha$ -helical antimicrobial peptides [11]. The peptide induces membrane permeabilization and lipid flip-flop via a toroidal pore consisting of peptide and lipid molecules [12,13].

In this study, PEG (M.W.=5000) was attached to the N-terminus of F5W, E19Q-magainin 2-amide (PEG-E19Q-MGa). The E19Q substitution and C-terminal amidation are expected to enhance antimicrobial activity by increasing positive charges [14]. Introduction of a Trp residue enables fluorometrical monitoring of peptide–membrane interaction. Ac-F5W, E19Q-magainin 2-amide (Ac-E19Q-MGa) was used as a control for PEG-E19Q-MGa. F5W-magainin 2 (MG), an equipotent analogue of magainin 2 [15], was also used as another control. We compared PEG-E19Q-MGa, Ac-E19Q-MGa, and MG (Fig. 1) in terms of conformation, membrane binding, antimicrobial activity, cytotoxicity against mammalian cells, and membrane-permeabilizing activity against liposomes and *Escherichia coli* ML-35. We also compared and discussed the effects of PEGylation on the activities of  $\alpha$ -helical magainin 2 and  $\beta$ -sheet tachyplesin I.

## 2. Materials and methods

### 2.1. Peptides

PEG-E19Q-MGa and Ac-E19Q-MGa were custom synthesized by Peptide Institute (Minou, Japan) and Toray Research Center (Tokyo, Japan), respectively. MG was synthesized by a standard Fmoc-based solid phase method as described elsewhere [15]. The concentrations of all peptides were determined on the basis of tryptophan UV absorption.

### 2.2. Liposomes

Egg yolk L- $\alpha$ -phosphatidylcholine (PC) and L- $\alpha$ -phosphatidyl-DL-glycerol enzymatically converted from PC (PG) were obtained from Sigma (St. Louis,

MG

GIGKWLHSAKKFGKAFVGEIMNS

PEG-E19Q-MGa

CH<sub>3</sub>-O-(CH<sub>2</sub>-CH<sub>2</sub>-O)<sub>n</sub>-C(=O)-CH<sub>2</sub>-CH<sub>2</sub>-C(=O)-GIGKWLHSAKKFGKAFVGEIMNS-amide

Ac-E19Q-MGa

Ac-GIGKWLHSAKKFGKAFVGEIMNS-amide

Fig. 1. Amino acid sequences of the peptides used in this study.

MO). Calcein was supplied by Dojindo (Kumamoto, Japan). The fluorescent lipid, 1-palmitoyl-2-[6-[(7-nitrobenz-2-oxa-1,3-diazol-4-yl) amino]caproyl]-L- $\alpha$ -phosphatidylcholine (C<sub>6</sub>-NBD-PC) was purchased from Molecular Probes (Eugene, OR). All other chemicals were of special grade and were obtained from Wako (Osaka, Japan).

The lipid composition of bacterial inner membranes significantly differs strain by strain. For example, the inner membrane of *Staphylococcus epidermidis* is mainly composed of PG, and *Pseudomonas carboxydovorans* contains PC. We have been using PG/PC (1/1) system as a model for bacterial inner membranes. A mixture of phosphatidylethanolamine and PG is often used to mimic the inner membrane of *E. coli*. Incorporation of phosphatidylethanolamine is expected to decrease membrane-permeabilizing activity of MG as shown in our previous study [16].

Large unilamellar vesicles (LUVs) were prepared and characterized, as previously described elsewhere [15]. Briefly, a lipid film, after being dried under vacuum overnight, was hydrated with a Tris buffer (10 mM Tris/150 mM NaCl/1 mM EDTA, pH 7.4) or a 70 mM calcein solution (pH was adjusted to 7.4 with 1 N NaOH) and vortexed. The suspension was freeze–thawed for 10 cycles to produce multilamellar vesicles (MLVs).

For CD measurements, small unilamellar vesicles (SUVs) were prepared by sonication of MLVs in ice/water under a nitrogen atmosphere.

MLVs used in translocation experiments were freeze–thawed only once to keep the lamellarity larger than 1. MLVs were then successively extruded through polycarbonate filters (a 100 nm pore size filter  $\times$  31 times) to obtain LUVs. Dye-entrapped vesicles were separated from free calcein on a Bio-Gel A-1.5 m column. The lipid concentration was determined by phosphorus analysis [17].

### 2.3. CD spectra

CD spectra were measured on a Jasco J-820 at 30 °C using a 1-mm path-length quartz cell to minimize the absorbance due to buffer components. Eight scans were averaged for each sample. The averaged blank spectra (the vesicle suspension) were subtracted. Spectra of the peptides in the membrane-bound form were recorded by use of PG/PC (1/1) SUVs. The peptide and the lipid concentrations were 25  $\mu$ M and 1.0 mM or 2.0 mM, respectively. The absence of any optical artifacts was confirmed elsewhere [18].

### 2.4. Calcein leakage

The release of calcein from the dye-entrapped LUVs was monitored fluorometrically on a Shimadzu RF-5300 spectrofluorometer at an excitation wavelength of 490 nm and at an emission wavelength of 520 nm at 30 °C. Calcein-free LUVs were mixed with dye-loaded liposomes to adjust the lipid concentration to the desired value. The maximum fluorescence intensity corresponding to 100% leakage was determined by addition of 10% (w/v) Triton X-100 (20  $\mu$ L) to 2 mL of the sample. The percentage of apparent leakage was calculated according to the relationship

$$\% \text{ of apparent leakage} = 100 \times (F - F_0)/(F_t - F_0)$$

where  $F$  and  $F_t$  are fluorescence intensities before and after addition of the detergent, respectively, and  $F_0$  represents the fluorescence of intact vesicles.

### 2.5. Peptide binding

The binding of the peptides to LUVs composed of PG/PC (1/1) was estimated on the basis of their Trp fluorescence [15]. Peptide solutions (4  $\mu$ M) were titrated with a vesicle suspension while the fluorescence spectra of the Trp residue were recorded after every 45-min incubation for equilibration. Fluorescence data were averaged for two independent samples after volume correction for dilution (up to 5%).

### 2.6. Lipid flip-flop

The peptide-induced lipid flip-flop was detected using NBD-labeled LUVs (PG/PC/C<sub>6</sub>-NBD-PC=50/49.5/0.5) and dithionite ion as previously reported

[12]. The symmetrically labeled vesicles were mixed with 1 M sodium dithionite/1 M Tris ([lipid]=40 mM, [dithionite]=60 mM) and incubated for 15 min at 30 °C to produce inner leaflet-labeled vesicles. The vesicles were immediately separated from free dithionite by gel filtration (Bio-Gel A1.5 m, 1.5×30 cm column). The fraction of NBD-lipids that had flopped during incubation in the absence or presence of the peptide was measured on the basis of fluorescence quenching by sodium dithionite. The asymmetrically NBD-labeled LUVs (2.0 mL) were incubated with or without the peptide for various periods at 30 °C. In the peptide-containing samples, 50  $\mu$ L of a trypsin solution (9.6 mg/mL) was added to 2-mL samples and reacted for 1 min to hydrolyze the peptide. After addition of 20  $\mu$ L of 1 M sodium dithionite/1 M Tris, NBD fluorescence was monitored with excitation and emission wavelengths of 460 and 530 nm, respectively. The percent flip-flop was calculated as described previously [12].

### 2.7. Peptide translocation

Translocation of the peptide into the inner leaflet of the bilayer was examined with the use of MLVs composed of PG/PC/C<sub>6</sub>-NBD-PC (50/49.5/0.5) [19]. Small aliquots of the MLVs were added to a peptide solution or to a buffer as the control in the presence of 10 mM sodium dithionite. The fluorescence intensity of NBD at 530 nm (excitation wavelength, 450 nm) was monitored at 30 °C. The intensity was represented relative to the value in the absence of the dithionite ion.

### 2.8. Antimicrobial activity

The minimum inhibitory concentrations (MICs) of the peptides were determined as described previously [20]. Briefly, *E. coli* (ATCC 25922) and *S. epidermidis* (ATCC 12228) were cultured in 3% (w/v) Tryptic soy broth (TSB) at 37 °C for 20 h. To obtain midlogarithmic phase microorganisms, 1-mL aliquots of the cultures were transferred to 100 mL of fresh TSB broth and incubated for 2–3 h. The cells were washed with 10 mM sodium phosphate/100 mM NaCl, pH 7.4 buffer (NAPB) and resuspended in the same buffer. The cell concentrations were estimated by measuring the absorbance at 600 nm (ABS<sub>600</sub>). The relationship between the cell concentration and ABS<sub>600</sub> was predetermined as (CFU/mL=ABS<sub>600</sub>×3.4×10<sup>8</sup>) for *E. coli* and (CFU/mL=ABS<sub>600</sub>×1.6×10<sup>8</sup>) for *S. epidermidis*. The suspensions were diluted to 4×10<sup>5</sup> CFU/mL. The inoculum (90  $\mu$ L) was added to each well of 96-well plates. The peptide samples (10  $\mu$ L) were added to each well and the plates were incubated at 37 °C for 3 h. TSB [6% (w/v), 100  $\mu$ L] was added, and the plates were incubated at 37 °C for 20 h. Cell growth was assessed by measuring the ABS<sub>595</sub> on a model 680 microplate reader (Bio-Rad, Hercules, CA). MIC was defined as the lowest concentration of the peptide that inhibited growth.

### 2.9. Cytotoxicity

2-(4-Iodophenyl)-3-(4-nitrophenyl)-5-(2,4-disulfophenyl)-2H-tetrazolium, monosodium salt (WST-1) was obtained from Roche Applied Science (Mannheim, Germany). Alpha modification of Eagle's medium (AMEM) was purchased from ICN Biomedicals (Aurora, OH). The cytotoxicity of the peptides against Chinese Hamster Ovary (CHO)-K1 cells was assessed using the WST-1 assay [21] according to the manufacturer's procedure. The cells (1×10<sup>4</sup>/well) in AMEM containing 10% fetal bovine serum (FBS) were cultured in 96-well microplates and incubated for 12 h under 5% CO<sub>2</sub> at 37 °C. After removal of the medium, the cells were incubated with 100  $\mu$ L of the peptide dissolved in the medium (100  $\mu$ M) for 24 h at 37 °C. Ten microliters of the WST-1 solution was added, and the cells were further incubated for 1 h. The percent cell viability was determined by (ABS<sub>450</sub>-ABS<sub>655</sub>) for the peptide-treated cells/(ABS<sub>450</sub>-ABS<sub>655</sub>) for the untreated cells×100. All measurements were made at least in triplicate.

### 2.10. Inner membrane permeability

*o*-Nitrophenyl- $\beta$ -D-galactoside (ONPG) was purchased from Aldrich (Milwaukee, WI). *E. coli* ML-35 (*i*<sup>-</sup>, *y*<sup>-</sup>, *z*<sup>+</sup>) strain was used to estimate the inner membrane-permeabilizing activity of the peptides based on the method of Lehrer [22]. The bacteria were resuspended in NAPB and adjusted to an ABS<sub>620</sub> value of 0.35 (~1×10<sup>8</sup> CFU/mL). The cells in 96-well plates were preincubated with ONPG in NAPB containing 1% TSB (v/v) at 37 °C for 60 min. The peptide

solution in NAPB was then added to each well, and absorbance at 405 nm was measured. The final concentrations of *E. coli* ML-35, ONPG, and the peptide were 1×10<sup>7</sup> CFU/mL, 1.67 mM, and 2  $\mu$ M, respectively. During the inner membrane permeability assay, CFU of bacteria was also monitored. At various time points, aliquots (10  $\mu$ L) were taken from the sample solution and diluted with the buffer solution (>100 fold) to stop the action of the peptides. Aliquots (100  $\mu$ L) of the diluted solution were seeded on Luria-Bertani agar plates and CFU were counted after 12 h.

## 3. Results

### 3.1. CD spectra

The secondary structure of PEG-E19Q-MGa was compared to that of Ac-E19Q-MGa and MG in the presence of 1 mM PG/PC SUVs (Fig. 2). Because further addition of SUVs did not change CD spectra (data not shown), the peptides were completely bound to SUVs under these conditions. All peptides conformed to helices as characterized by double minima at 208–209 and 222 nm and a maximum below 200 nm. The  $[\theta]_{222}$  values were -15000, -21700 and -26000 deg cm<sup>2</sup> dmol<sup>-1</sup> for PEG-E19Q-MGa, MG and Ac-F5W-E19Q-MGa, respectively, indicating that in terms of helicity estimated according to Chen et al. [23], the order was PEG-E19Q-MGa (41.7%)<MG (63.9%)<Ac-E19Q-MGa (78.0%).

### 3.2. Leakage activity

To investigate whether PEGylation alters the activity of the parent peptide against liposomes or not, we compared the membrane permeabilizing activities of the peptides. Fig. 3 shows the time course of leakage of the fluorescent dye from PG/PC LUVs mimicking bacterial cell membranes. With respect to leakage activity, the order was Ac-E19Q-MGa≈MG>PEG-E19Q-MGa. An equivalent amount of PEG per se was confirmed to have no effect on the membrane-permeabilizing activities of MG or Ac-E19Q-MGa (data not shown).

### 3.3. Binding affinity

The binding affinity of the peptides for PG/PC membranes was estimated on the basis of changes in tryptophan fluorescence

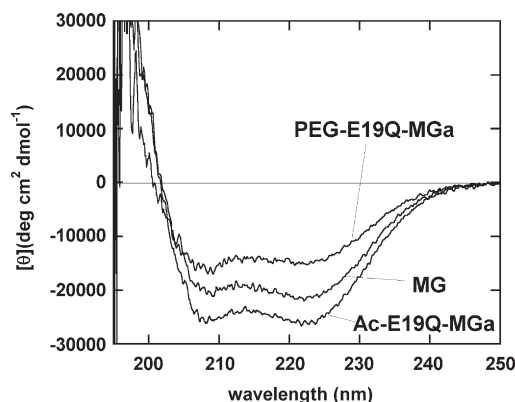


Fig. 2. CD spectra. The CD spectra of the peptides (25  $\mu$ M) were measured at 30 °C in 1 mM PG/PC (1/1) SUVs.

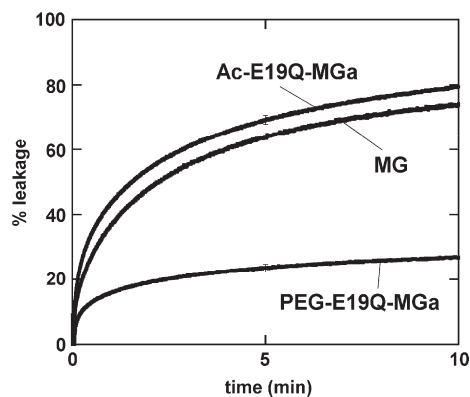


Fig. 3. Membrane-permeabilizing activity of the peptides at 30°C. The percent leakage value of calcein is plotted as a function of time. PG/PC (1/1) LUVs. [peptide]=0.8  $\mu$ M. [lipid]=54.5  $\mu$ M.

upon binding. Fig. 4 shows the wavelength of maximal intensity,  $\lambda_{\max}$  (A), and the intensity enhancement at 336 nm (B) as a function of the lipid-to-peptide molar ratio (L/P). In the absence of PG/PC liposomes, MG taking an unordered structure [24] showed a peak at 352 nm, indicating the Trp residue is exposed to the aqueous phase. PEG-E19Q-MGa and Ac-E19Q-MGa showed spectra superimposable on that of MG (spectra not shown), suggesting that there is no interaction between the tryptophan residue of PEG-E19Q-

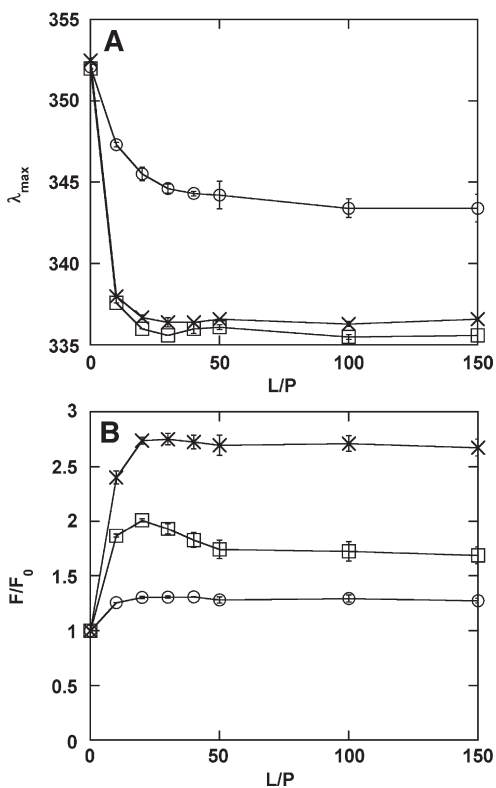


Fig. 4. Changes in tryptophan fluorescence of the peptides upon binding to PG/PC (1/1) LUVs at 30 °C. The wavelength of maximal intensity  $\lambda_{\max}$  (A) and the fluorescence intensity at 336 nm (B) are plotted as a function of L/P ([peptide]=4.0  $\mu$ M). The excitation wavelength was 280 nm. Peptides: squares, MG; circles, PEG-E19Q-MGa; crosses, Ac-E19Q-MGa.

MGa and the PEG moiety in contrast to the case of PEG-tachyplesin [9]. The addition of LUVs caused a blue shift and a simultaneous intensity enhancement, indicating that the fluorophore is buried in a hydrophobic environment of the membrane [15]. PEG-E19Q-MGa showed a smaller blue shift than the other two peptides, indicating that the peptide penetrates less deeper into the bilayer. MG and Ac-E19Q-MGa showed similar changes in  $\lambda_{\max}$ . The binding of the latter two peptides was obviously saturated at lower L/P values than that of PEG-E19Q-MGa, indicating the lower binding affinity of PEG-E19Q-MGa. However, all peptides were almost completely bound to PG/PC membranes at L/P=68.1 in the leakage experiments. In enhancement in fluorescence, the order was Ac-E19Q-MGa>MG>PEG-E19Q-MGa. For MG, the intensity at L/P values below 50 was larger than the saturated value, as reported previously [15]. This abnormal behavior was suggested to be due to the dimerization of MG [26].

### 3.4. Lipid flip-flop

We assessed the lipid flip-flop induced by the peptides using a combination of NBD-PC and dithionite ions [12] (Fig. 5). Our laboratory has reported that MG induces lipid flip-flop coupled to pore formation [12]. PEG-E19Q-MGa (Fig. 5A) and Ac-E19Q-MGa (Fig. 5B) also induced the transbilayer movement

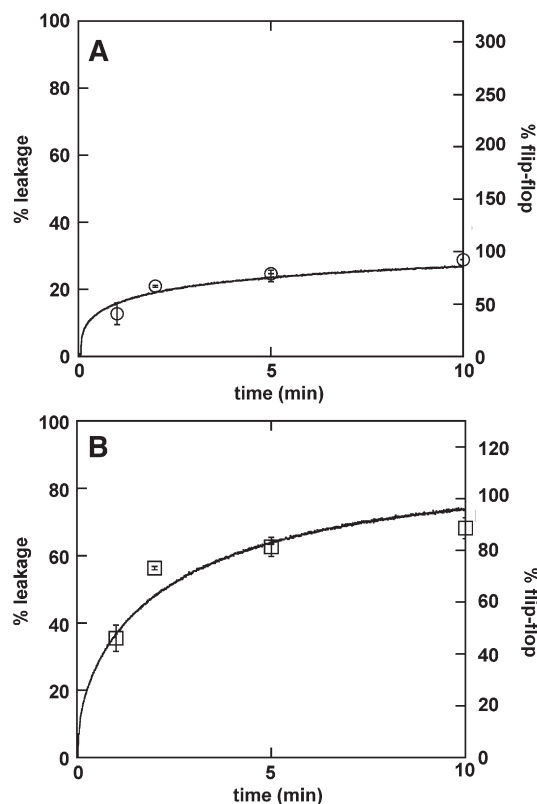


Fig. 5. Coupling between dye leakage and lipid flip-flop. Time courses of calcein leakage reproduced from Fig. 3 and lipid flip-flop are shown with traces and symbols, respectively, for (A) PEG-E19Q-MGa, and (B) Ac-E19Q-MGa. The lipid composition was PG/PC (1/1) for leakage experiments and 0.5 mol% C<sub>6</sub>-NBD-PC was included for lipid flip-flop measurements. [L]=54.5  $\mu$ M, [P]=0.8  $\mu$ M.

of the fluorescent lipid coupled to dye leakage. It should be noted that PEG-E19Q-MGa and Ac-E19Q-MGa induced flip-flop of a similar extent, although the leakage activity of PEG-E19Q-MGa was weaker.

### 3.5. Peptide translocation

With the conventional approach [25], the fluorescence resonance energy transfer between tryptophan residues in peptides and dansyl-labeled lipids incorporated into LUVs is used to quantify the fraction of membrane-bound peptide. However, the fluorescence energy transfer between the tryptophan residue of PEG-E19Q-MGa and dansyl-labeled lipids was not observed because of different fluorescence properties (Fig. 4). Therefore, the MLV method [19] was used instead to estimate the translocation of the peptides across lipid bilayers (Fig. 6). The addition of the reducing ion dithionite to MLVs containing NBD-PC reduced the NBD moieties exposed to the external aqueous phase, making them nonfluorescent. The decrease in fluorescence, corresponding to the fraction of the chromophores on the MLV surface, was about 23%, indicating that the lamellarity of the vesicles is larger than 2. If the peptides permeabilize only the outermost bilayers without translocation, the reducing ion can react with the NBD moieties facing the first interlamellar space, resulting in quenching of less than 69 ( $23 \times 3$ )%. The expected time course of quenching in this case is shown as the calculated curve in Fig. 6. In contrast, if the peptide translocates, it can permeabilize not only the outermost bilayers but also the inner bilayers, resulting in quenching of more than 69%. In this case, experimental quenching curves should be below the calculated curve. The quenching curves of PEG-E19Q-MGa, MG, and Ac-E19Q-MGa were below the calculated curve at concentrations of 4.0, 1.0, and 2.0  $\mu\text{M}$ , respectively, indicating all peptides translocate across bilayers. It should be noted that this experiment can only examine qualitatively whether a peptide can translocate or not.

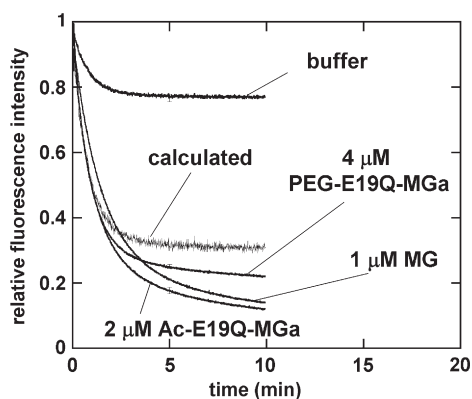


Fig. 6. Detection of translocation of the peptides at 30 °C. Small aliquots of MLVs composed of PG/PC/C<sub>6</sub>-NBD-PC (50/49.5/0.5) were injected into a buffer or a peptide solution in the presence of 10 mM sodium dithionite. The fluorescence (excitation at 450 nm, emission at 530 nm) was normalized to the intensity in the absence of the quencher. The calculated trace is the curve in the case of no translocation. [lipid]=100  $\mu\text{M}$ .

Table 1  
MICs of the peptides ( $\mu\text{M}$ )

|              | <i>E. coli</i><br>(ATCC25922) | <i>S. epidermidis</i><br>(ATCC12228) |
|--------------|-------------------------------|--------------------------------------|
| MG           | 20                            | 20                                   |
| PEG-E19Q-MGa | 80                            | 80                                   |
| AC-E19Q-MGa  | 20                            | 20                                   |

### 3.6. Biological activities

Table 1 summarizes the MIC values of the peptides against Gram-negative *E. coli* and Gram-positive *S. epidermidis*. MG and Ac-E19Q-MGa exhibited identical activities against both types of bacteria. The PEGylated peptide showed 4-fold weaker antimicrobial activity against both bacteria than the non-PEGylated peptides, although the PEGylated peptide has the same net charge as Ac-E19Q-MGa.

We then assessed the cytotoxicity of the peptides against mammalian CHO-K1 cells (Table 2). At a concentration of 100  $\mu\text{M}$ , the non-PEGylated peptides were highly toxic. The cell viability was close to zero. In contrast, PEG-E19Q-MGa was nontoxic.

### 3.7. Inner membrane permeability

To investigate why antimicrobial activity was decreased by PEGylation, we compared the inner membrane-permeabilizing activities of the peptides using *E. coli* ML-35 cells which lack lactose permease necessary for the uptake of ONPG. If the peptide induces the permeabilization of inner membranes, ONPG enters the cytoplasm and is degraded by  $\beta$ -galactosidase, producing *o*-nitrophenol that shows absorbance at 405 nm. The PEGylated peptide neither induced the permeabilization of inner membranes nor decreased the viability of bacteria during 60 min (Fig. 7). In contrast, MG induced a rapid increase in the permeability of inner membranes, concomitant with a rapid decrease in viability (Fig. 7), suggesting that the membrane-permeabilizing activity mainly contributed to the bacterial killing activity of MG.

## 4. Discussion

### 4.1. Effect of PEGylation on magainin 2-membrane interactions

CD spectra (Fig. 2) showed that the PEGylation lowered the helicity of magainin in the bilayer. The N-terminal hydrophilic PEG moiety appears to prevent the N-terminus from being

Table 2  
Cytotoxicity of the peptides against CHO-K1 cells

|              | Cell viability (%)<br>at 100 $\mu\text{M}$ |
|--------------|--------------------------------------------|
| MG           | 0.5 $\pm$ 1.7                              |
| PEG-E19Q-MGa | 96.6 $\pm$ 5.5                             |
| AC-E19Q-MGa  | 5.6 $\pm$ 8.9                              |

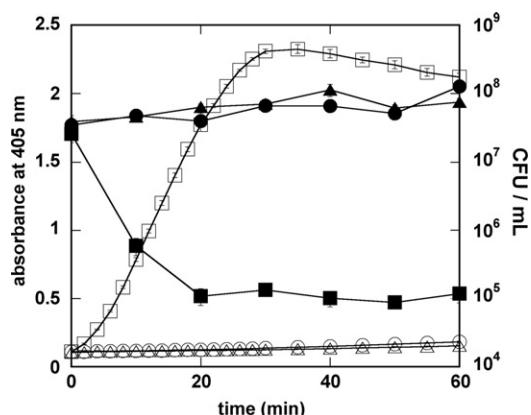


Fig. 7. Inner membrane permeabilization against *E. coli* ML-35 at 25 °C. Absorbance at 405 nm of MG-(square), PEG-E19Q-MG-(circle), and buffer-(triangle) treated cells is shown as a function of time. [peptide]=20  $\mu$ M. The viability of bacteria (CFU/mL) is also shown with the corresponding closed symbols.

inserted into the membrane, leading to the lower helicity and the shallower insertion depth of the PEGylated peptide (Fig. 4). Although PEGylation does not alter the secondary structure of insulin [27], tachyplesin I [9], or interferon  $\alpha$ -2b [28], these proteins are stabilized by intramolecular disulfide bonds. In contrast, Ac-E19Q-MGa exhibited the highest helicity, which is ascribable to the stabilization of the helix in the N-terminal region through elimination of the electrostatic repulsion between the positively-charged N-terminus and the helix macro dipole [29].

The binding affinity of the PEGylated peptide for PG/PC membranes was weaker than those of the non-PEGylated peptides (Fig. 4A). In addition to the lower helicity and the shallower penetration, the charge-masking effect of the PEG moiety [30] may also contribute to the lower binding affinity. PEGylation also lowered the binding affinity of tachyplesin I [9]. However, the decrease in affinity is more prominent for MG than for tachyplesin I, because the depth of tachyplesin I in the membrane does not change upon PEGylation.

The binding affinity of Ac-E19Q-MGa with larger positive charges was almost the same as that of MG (Fig. 4A) probably because of two opposing factors, i.e., the enhanced electrostatic interaction and the enhanced helicity of Ac-E19Q-MGa. The former increases the binding affinity. We have reported that F10W, E19Q-magainin 2-amide with +5 charges showed enhanced affinity for PG/PC membranes compared to F10W-magainin 2 with +3 charges [24]. On the other hand, the increased helicity may lead to a decrease in binding affinity because one peptide molecule induces a large positive curvature strain to membranes, thereby destabilizing the peptide–lipid system. No increase in helicity was observed for F10W, E19Q-magainin 2-amide [24].

The  $\lambda_{\max}$  value of Ac-E19Q-MGa was almost the same as that of MG, indicating similar locations in the membrane (Fig. 4A). However, the extent of enhancements in the presence of membranes was quite different (Fig. 4B). The protonated amino group is known to be an effective quencher for tryptophan [31].

The attachment of the large PEG moiety (5 kDa) to the smaller parent peptide (2.5 kDa) weakened the intrinsic leakage activity (Fig. 3), partly because the PEGylated peptide could not efficiently induce a positive curvature strain required for forming toroidal pores due to the lower helicity and the shallower insertion. Another possibility is that the PEG moiety, which is more extruded into the aqueous phase compared to the case of the PEGylated tachyplesin I [9], could clog the pore. Indeed, the leakage-to-flip-flop ratio of PEG-E19Q-MGa was smaller than that of the acetylated counterpart (Fig. 5). Ac-E19Q-MG, whose depth in the membrane was almost the same as that of MG (Fig. 4A), showed very similar membrane-permeabilizing activity to MG against PG/PC LUVs (Fig. 3). We have reported that the charge-enhanced peptide F10W, E19Q-magainin 2-amide had less membrane-permeabilizing activity than F10W-magainin 2 due to the instability of the pore [24]. In the current case, the pore destabilization caused by the increased charge appears to be compensated for by increased pore-forming activity due to the enhanced helicity (vide supra). Unlike with magainin, PEGylation did not alter the depth of insertion and therefore membrane-permeabilizing activity of tachyplesin I [9].

The PEGylated peptide was translocated into the inner leaflet of the bilayer (Fig. 6). The efficiency of NBD quenching depends on several factors other than the translocating activity, i.e., the binding affinity of each peptide for membranes and the membrane permeabilization activity. The apparent reduced translocation ability of the PEGylated peptide is at least partly due to the smaller binding affinity (Fig. 4) and the weaker membrane-permeabilizing activity against PG/PC (Fig. 3). The L/P value for the outermost bilayers was smaller than 25, where the PEGylated peptide did not bind completely to the membrane (Fig. 4A).

#### 4.2. Effect of PEGylation on biological activities

The non-PEGylated peptides were highly toxic to CHO-K1 cells at a concentration of 100  $\mu$ M, whereas PEGylation nullified the cytotoxicity (Table 2). The charge-masking effect may contribute to the diminished toxicity. It is also possible that the PEGylated peptide could not permeate the extracellular matrix efficiently due to large steric hindrance of the PEG moiety. PEGylation also lowered the cytotoxicity of tachyplesin I [9].

Not only cytotoxicity but also antimicrobial activity was reduced by PEGylation (Table 1). PEGylation has been reported to decrease the antimicrobial activity of tachyplesin I [9], nisin [8], and  $\alpha$ -defensin [32]. However, the extent of the reduction is strongly dependent on the peptide. In the case of the magainin analogue, the decrease was only 4-fold. The decrease is ascribable to the existence of outer membranes and peptidoglycan layers, as discussed elsewhere [9]. The smaller binding affinity and the weaker membrane-permeabilizing activity against PG/PC LUVs of the PEGylated peptide (Fig. 4A) could also contribute to the weaker antimicrobial activity. In contrast, the decrease in antimicrobial

activity by PEGylation is more prominent for tachyplesin I (32–64 fold). The mechanism of antimicrobial action of tachyplesin I may involve binding to bacterial DNA [33], although we have reported that membrane permeabilization contributes mainly. The impairment of the membrane-permeabilizing activity and DNA binding by PEGylation could lead to the larger decrease in antimicrobial activity of tachyplesin I.

## 5. Conclusion

We designed a PEGylated peptide based on the  $\alpha$ -helical antimicrobial peptide magainin 2 and examined the effects of PEGylation on the mechanism of membrane permeabilization of the peptide. The results were compared to those for the PEGylated  $\beta$ -sheet tachyplesin I. The attachment of a large PEG moiety (5 kDa) lowers the membrane binding for both peptides. A reduction in membrane-permeabilizing activity occurs only for magainin, because the PEGylation destabilizes the secondary structure. However, the PEGylation does not change the essential mode of action against lipid bilayers. The PEGylation significantly reduces cytotoxicity and the antimicrobial activity at the same time. The extent of the decrease depends on the peptide.

## Acknowledgements

This work was supported by Grant-in-Aids for Scientific Research (17651125) from the Ministry of Education, Culture, Sports, Science and Technology of Japan, and the 21st Century COE Programs “Knowledge Information Infrastructure for Genome Science” and “Initiatives for Attractive Education in Graduate Schools”.

## References

- [1] M. Zasloff, Antimicrobial peptides of multicellular organisms, *Nature* 415 (2002) 389–395.
- [2] K.A. Brogden, Antimicrobial peptides: pore formers or metabolic inhibitors in bacteria? *Nat. Rev., Microbiol.* 3 (2005) 238–250.
- [3] R.E. Hancock, H.G. Sahl, Antimicrobial and host-defense peptides as new anti-infective therapeutic strategies, *Nat. Biotechnol.* 24 (2006) 1551–1557.
- [4] J.M. Harris, R.B. Chess, Effect of PEGylation on pharmaceuticals, *Nat. Rev., Drug Discov.* 2 (2003) 214–221.
- [5] D.A. Steinberg, M.A. Hurst, C.A. Fujii, A.H. Kung, J.F. Ho, F.C. Cheng, D.J. Loury, J.C. Fiddes, Protegrin-1: a broad-spectrum, rapidly microbicidal peptide with *in vivo* activity, *Antimicrob. Agents Chemother.* 41 (1997) 1738–1742.
- [6] R.P. Darveau, M.D. Cunningham, C.L. Seachord, L. Cassiano-Clough, W.L. Cosand, J. Blake, C.S. Watkins, Beta-lactam antibiotics potentiate magainin 2 antimicrobial activity *in vitro* and *in vivo*, *Antimicrob. Agents Chemother.* 35 (1991) 1153–1159.
- [7] I. Ahmad, W.R. Perkins, D.M. Lupan, M.E. Selsted, A.S. Janoff, Liposomal entrapment of the neutrophil-derived peptide indolicidin endows it with *in vivo* antifungal activity, *Biochim. Biophys. Acta* 1237 (1995) 109–114.
- [8] A. Guiotto, M. Pozzobon, M. Canevari, R. Manganelli, M. Scarin, F.M. Veronese, PEGylation of the antimicrobial peptide nisin A: problems and perspectives, *Il Farmaco* 58 (2003) 45–50.
- [9] Y. Imura, M. Nishida, Y. Ogawa, Y. Takakura, K. Matsuzaki, Action mechanism of tachyplesin I and effects of PEGylation, *Biochim. Biophys. Acta* 1768 (2007) 1160–1169.
- [10] M. Zasloff, Magainins, a class of antimicrobial peptides from *Xenopus* skin: isolation, characterization of two active forms, and partial cDNA sequence of a precursor, *Proc. Natl. Acad. Sci. U. S. A.* 84 (1987) 5449–5453.
- [11] K. Matsuzaki, Magainins as paradigm for the mode of action of pore forming polypeptides, *Biochim. Biophys. Acta* 1376 (1998) 391–400.
- [12] K. Matsuzaki, O. Murase, N. Fujii, K. Miyajima, An antimicrobial peptide, magainin 2, induced rapid flip-flop of phospholipids coupled with pore formation and peptide translocation, *Biochemistry* 35 (1996) 11361–11368.
- [13] S.J. Ludtke, K. He, W.T. Heller, T.A. Harroun, L. Yang, H.W. Huang, Membrane pores induced by magainin, *Biochemistry* 35 (1996) 13723–13728.
- [14] K. Matsuzaki, K. Sugishita, M. Harada, N. Fujii, K. Miyajima, Interactions of an antimicrobial peptide, magainin 2, with outer and inner membranes of Gram-negative bacteria, *Biochim. Biophys. Acta* 1327 (1997) 119–130.
- [15] K. Matsuzaki, O. Murase, H. Tokuda, S. Funakoshi, N. Fujii, K. Miyajima, Orientational and aggregational states of magainin 2 in phospholipid bilayers, *Biochemistry* 33 (1994) 3342–3349.
- [16] K. Matsuzaki, K. Sugishita, N. Ishibe, M. Ueha, S. Nakata, K. Miyajima, R.M. Epand, Relationship of membrane curvature to the formation of pores by magainin 2, *Biochemistry* 37 (1998) 11856–11863.
- [17] G.R. Bartlett, Phosphorus assay in column chromatography, *J. Biol. Chem.* 234 (1959) 466–468.
- [18] K. Matsuzaki, S. Nakai, T. Handa, Y. Takaishi, T. Fujita, K. Miyajima, Hypelcin A, an alpha-aminoisobutyric acid containing antibiotic peptide, induced permeability change of phosphatidylcholine bilayers, *Biochemistry* 28 (1989) 9392–9398.
- [19] K. Matsuzaki, S. Yoneyama, K. Miyajima, Pore formation and translocation of melittin, *Biophys. J.* 73 (1997) 831–838.
- [20] S. Kobayashi, K. Takeshima, C.B. Park, S.C. Kim, K. Matsuzaki, Interactions of the novel antimicrobial peptide buforin 2 with lipid bilayers: proline as a translocation promoting factor, *Biochemistry* 39 (2000) 8648–8654.
- [21] M. Ishiyama, M. Shiga, K. Sasamoto, M. Mizoguchi, P.G. He, A new sulfonated tetrazolium salt that produces a highly water-soluble formazan dye, *Chem. Pharm. Bull.* 41 (1993) 1118–1122.
- [22] R.I. Lehrer, A. Barton, K.A. Daher, S.S. Harwig, T. Ganz, M.E. Selsted, Interaction of human defensins with *Escherichia coli*. Mechanism of bactericidal activity, *J. Clin. Invest.* 84 (1989) 553–561.
- [23] Y.H. Chen, J.T. Yang, H.M. Martinez, Determination of the secondary structures of proteins by circular dichroism and optical rotatory dispersion, *Biochemistry* 11 (1972) 4120–4131.
- [24] K. Matsuzaki, A. Nakamura, O. Murase, K. Sugishita, N. Fujii, K. Miyajima, Modulation of magainin 2-lipid bilayer interactions by peptide charge, *Biochemistry* 36 (1997) 2104–2111.
- [25] K. Matsuzaki, O. Murase, N. Fujii, K. Miyajima, Translocation of a channel-forming antimicrobial peptide, magainin 2, across lipid bilayers by forming a pore, *Biochemistry* 34 (1995) 6521–6526.
- [26] K. Matsuzaki, Y. Mitani, K.Y. Akada, O. Murase, S. Yoneyama, M. Zasloff, K. Miyajima, Mechanism of synergism between antimicrobial peptides magainin 2 and PGLa, *Biochemistry* 37 (1998) 15144–15153.
- [27] K.D. Hinds, K.M. Campbell, K.M. Holland, D.H. Lewis, C.A. Piche, P.G. Schmidt, PEGylated insulin in PLGA microparticles. *In vivo* and *in vitro* analysis, *J. Control. Release* 104 (2005) 447–460.
- [28] Y.S. Wang, S. Youngster, M. Grace, J. Bausch, R. Bordens, D.F. Wyss, Structural and biological characterization of pegylated recombinant interferon alpha-2b and its therapeutic implications, *Adv. Drug Deliv. Rev.* 54 (2002) 547–570.
- [29] K.R. Shoemaker, P.S. Kim, E.J. York, J.M. Stewart, R.L. Baldwin, Tests of the helix dipole model for stabilization of alpha-helices, *Nature* 326 (1987) 563–567.
- [30] M. Ogris, S. Brunner, S. Schuller, R. Kircheis, E. Wagner, PEGylated DNA/transferrin-PEI complexes: reduced interaction with blood

- components, extended circulation in blood and potential for systemic gene delivery, *Gene Ther.* 6 (1999) 595–605.
- [31] J.R. Lakowicz, *Principles of Fluorescence Spectroscopy*, Second edition, Kluwer Academic/Plenum Publishers, New York, 1999, Chapter 17.
- [32] Z. Wu, X. Li, B. Ericksen, E. de Leeuw, G. Zou, P. Zeng, C. Xie, C. Li, J. Lubkowski, W.Y. Lu, W. Lu, Impact of pro segments on the folding and function of human neutrophil alpha-defensins, *J. Mol. Biol.* 368 (2007) 537–549.
- [33] A. Yonezawa, J. Kuwahara, N. Fujii, Y. Sugiura, Binding of tachyplesin I to DNA revealed by footprinting analysis: significant contribution of secondary structure to DNA binding and implication for biological action, *Biochemistry* 31 (1992) 2998–3004.